LETTERS
PUBLISHED ONLINE: 2 SEPTEMBER 2012 | DOI: 10.1038/NMAT3409

nature materials

Spin excitations in a single La_2CuO_4 layer

M. P. M. Dean[1*], R. S. Springell[2,3], C. Monney[4], K. J. Zhou[4†], J. Pereiro[1†], I. Božović[1], B. Dalla Piazza[5], H. M. Rønnow[5], E. Morenzoni[6], J. van den Brink[7], T. Schmitt[4] and J. P. Hill[1*]

Cuprates and other high-temperature superconductors consist of two-dimensional layers that are crucial to their properties. The dynamics of the quantum spins in these layers lie at the heart of the mystery of the cuprates[1–7]. In bulk cuprates such as La_2CuO_4, the presence of a weak coupling between the two-dimensional layers stabilizes a three-dimensional magnetic order up to high temperatures. In a truly two-dimensional system however, thermal spin fluctuations melt long-range order at any finite temperature[8]. Here, we measure the spin response of isolated layers of La_2CuO_4 that are only one-unit-cell-thick. We show that coherent magnetic excitations, magnons, known from the bulk order, persist even in a single layer of La_2CuO_4, with no evidence for more complex correlations such as resonating valence bond correlations[9–11]. These magnons are, therefore, well described by spin-wave theory (SWT). On the other hand, we also observe a high-energy magnetic continuum in the isotropic magnetic response that is not well described by two-magnon SWT, or indeed any existing theories.

The simplest model for describing the magnetic excitations of undoped cuprates is SWT (ref. 12). Coherent transverse magnetic excitations correspond to spin waves—magnons—with a well-defined energy; whereas longitudinal magnetic excitations result in a high-energy continuum of multi-magnons. Although measurements of the long-wavelength magnetic excitations of La_2CuO_4 (ref. 13) can be understood in terms of a renormalized classical model[14], the short-range correlations remain controversial[6,9,10,15–17] as quantum fluctuations can transfer spectral weight out of the magnon peak into a high-energy continuum. Furthermore, the magnetic excitation spectrum of a one-unit-cell-thick (1 uc) La_2CuO_4 layer containing two CuO_2 planes, where spin fluctuations are expected to be enhanced, has not been measured. This is because most of what we know about the spin excitation spectrum of the cuprates has come from inelastic neutron scattering. Unfortunately, such experiments require large samples and are often challenging at high-energy transfers. In recent years, however, resonant inelastic X-ray scattering (RIXS) has achieved sufficient resolution to access magnetic excitations[7,18–21] and RIXS is well suited to measuring high-energy magnetic excitations in the range 100–1,000 meV. Furthermore, the high sensitivity of the technique allows us to look at nanostructured samples and this in turn opens up the exciting possibility of measuring the spin response of a 1 uc La_2CuO_4 layer for the first time.

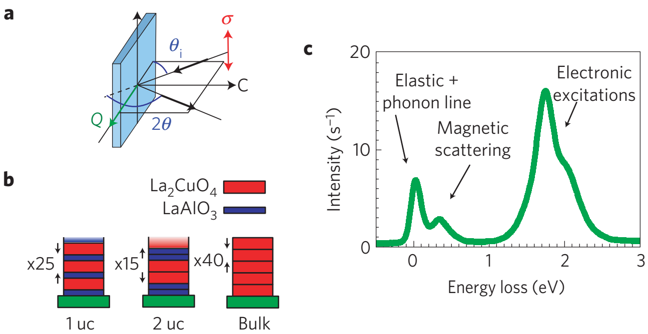

Figure 1 | The scattering geometry, a schematic of the samples and a typical RIXS spectrum. a, The experimental scattering geometry. The 931 eV σ-polarized X-rays are incident at an angle θ_i and are scattered through a fixed angle $2\theta = 130°$. Large **Q** corresponds to near-grazing incidence ($\theta_i \to 0$). **b**, The multilayer films studied, composed of 13.2 Å La_2CuO_4 layers (red blocks) containing two CuO_2 planes and 3.8 Å $LaAlO_3$ (blue blocks). We label the films, on the basis of the thickness of La_2CuO_4, as 1 uc, 2 uc and bulk. The arrows denote the repeat unit of the films (×25, ×15, ×40). **c**, A representative RIXS spectrum of the 1 uc La_2CuO_4 film ($25 \times [LaAlO_3 + La_2CuO_4]$) at $\mathbf{Q} = (0.77\pi, 0)$ identifying the main spectral features: the elastic and phonon scattering around zero-energy transfer, the magnetic scattering around 300 meV and the electronic (*dd*) excitations from 1 to 3 eV.

We performed RIXS measurements on bulk and single-layer La_2CuO_4 films at 15 K using the scattering geometry shown in Fig. 1a. The sample was rotated about the vertical axis to vary **Q**, the projection of the total scattering vector in the *ab* plane. To provide a sufficient scattering volume of isolated La_2CuO_4 layers, we prepared heterostructures based on 1 uc layers of La_2CuO_4 and $LaAlO_3$. Note that 1 uc of La_2CuO_4 contains two CuO_2 layers. The samples are depicted in Fig. 1b as 1 uc = [1 uc $LaAlO_3$ + 1 uc La_2CuO_4] × 25, 2 uc = [2 uc $LaAlO_3$ + 2 uc La_2CuO_4] × 15, and bulk = [1 uc La_2CuO_4] × 40. The films were characterized using muon spin rotation (see Supplementary Information for a discussion). These results, and the RIXS results (discussed later), show that the correlated patches of spins are randomly orientated as might be expected for an isolated La_2CuO_4 layer.

The RIXS spectra of the three samples were measured from $(0.14\pi, 0)$ to $(0.8\pi, 0)$ and $(0.1\pi, 0.1\pi)$ to $(0.6\pi, 0.6\pi)$. Figure 1c

[1]Department of Condensed Matter Physics and Materials Science, Brookhaven National Laboratory, Upton, New York 11973, USA, [2]London Centre for Nanotechnology and Department of Physics and Astronomy, University College London, London WC1E 6BT, UK, [3]Royal Commission for the Exhibition of 1851 Research Fellow, Interface Analysis Centre, University of Bristol, Bristol BS2 8BS, UK, [4]Swiss Light Source, Paul Scherrer Institut, CH-5232 Villigen PSI, Switzerland, [5]Laboratory for Quantum Magnetism, École Polytechnique Fédérale de Lausanne (EPFL), CH-1015, Switzerland, [6]Laboratory for Muon Spin Spectroscopy, Paul Scherrer Institut, 5232 Villigen PSI, Switzerland, [7]Institute for Theoretical Solid State Physics, IFW Dresden, D01171 Dresden, Germany. †Present addresses: Diamond Light Source, Harwell Science and Innovation Campus, Didcot OX11 0DE, UK (K.J.Z.); Department of Physics, University of California, San Diego, La Jolla, California 92093, USA (J.P.). *e-mail: mdean@bnl.gov; hill@bnl.gov.

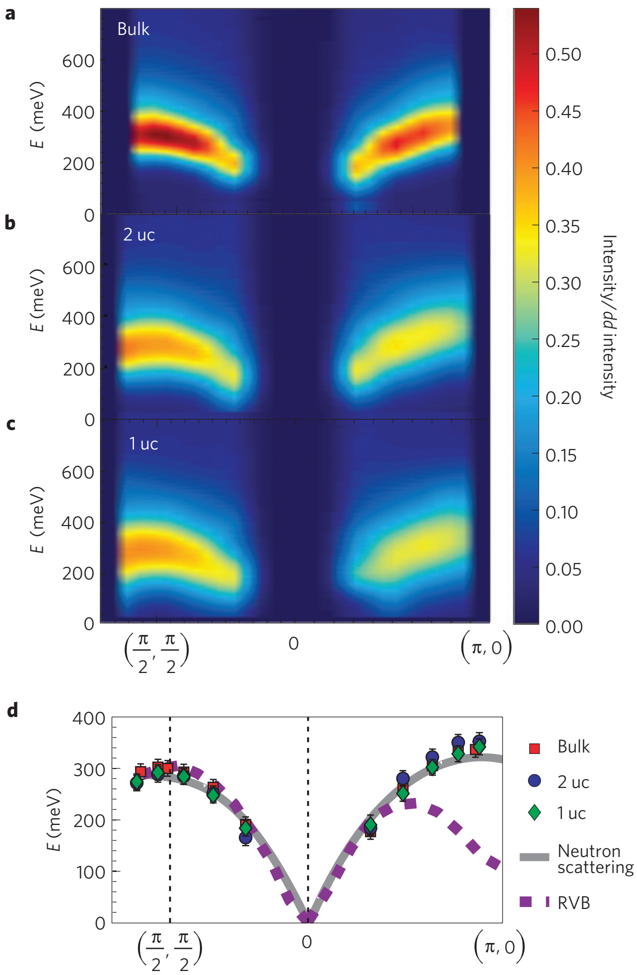

Figure 2 | Magnetic dispersions of isolated and coupled La_2CuO_4 layers. **a–c**, The magnetic RIXS scattering intensity at 15 K along the high-symmetry lines in the Brillouin zone for: (**a**) bulk film, (**b**) 2 uc ($15 \times [2LaAlO_3 + 2La_2CuO_4]$) and (**c**) 1 uc ($25 \times [LaAlO_3 + La_2CuO_4]$) samples. **d**, The peak energy dispersion in bulk (red squares), 2 uc (blue circles) and 1 uc La_2CuO_4 (green diamonds). The solid grey line is the result from neutron scattering measurements of bulk La_2CuO_4 (ref. 6); the dotted purple line are calculations for an RVB model[11].

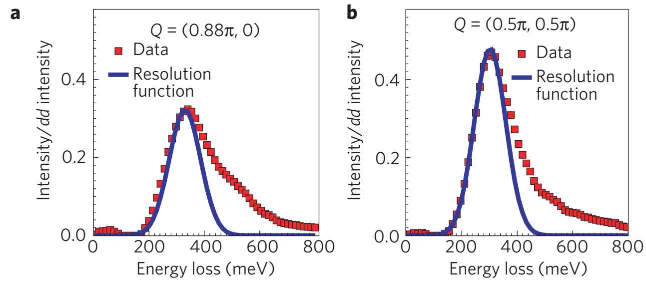

Figure 3 | Magnon peak showing anisotropic high-energy magnetic scattering. a,b, The measured magnetic spectral weight (red squares) in bulk La_2CuO_4 at $\mathbf{Q} = (0.88\pi, 0)$ (**a**) and $\mathbf{Q} = (0.5\pi, 0.5\pi)$ (**b**). The blue line is a resolution-limited Gaussian at the single-magnon energy. The statistical error bars are smaller than the point size.

plots a representative spectrum collected at $\mathbf{Q} = (0.77\pi, 0)$. We observe a peak corresponding to elastic scattering around zero-energy transfer, which also contains a shoulder at low-energy transfers (up to ~90 meV) due to phonon scattering. From 200 to 800 meV we observe magnetic scattering, and in the 1–3 eV window we identify electronic *dd* excitations.

The elastic and phonon peaks in the spectra were fitted using Gaussian functions and subtracted from the data, to isolate the magnetic scattering. In the bulk film the response is dominated by a dispersing magnon peak (see Fig. 2a), along with additional scattering extending out to higher energies. As $\mathbf{Q} \to 0$ the specular reflection from the sample surface overwhelms any magnetic signal. For the case of the 1 uc and 2 uc films, shown in Fig. 2b,c, the peak intensity is suppressed and the peak width is broadened with more weight at high energies.

Figure 2d plots the dispersion of the peak in the magnetic response of the three films. We see that the 1 uc and 2 uc films still exhibit a coherent magnon peak, with the same dispersion as in the bulk. For comparison we also plot neutron scattering results from bulk La_2CuO_4 (ref. 6). These are in excellent agreement along (0, 0) to $(\pi/2, \pi/2)$. Along (0, 0) to $(\pi, 0)$ our results seem slightly higher in energy than ref. 6. We attribute this to the fact that in the present case we are recording the median energy of the asymmetric peak, rather than the peak energy position, as is the case in ref. 6. This difference has a bigger effect along the $(\pi, 0)$ direction because of the increased high-energy tail in this direction, a fact that we will return to later.

Figure 2d shows the principal result of this paper: even in La_2CuO_4 layers only a single unit cell thick, a coherent, bulk-like magnon is a reasonable description of the magnetic excitations and this magnon can be probed by RIXS. Significantly, the dispersion is very similar to that of bulk La_2CuO_4. Thus, even though SWT is based on an ordered Néel state, it continues to provide a reasonable description of the spin response of a 1 uc La_2CuO_4 layer. This is despite the fact that the Néel-ordered state is predicted to be suppressed in the limiting case of an isolated two-dimensional Heisenberg antiferromagnet[14].

This is an important result. Recent muon spin rotation data seem to indicate that thin La_2CuO_4 layers are dominated by quantum fluctuations[17]. Indeed, calculations suggest that quantum fluctuations may be enhanced in La_2CuO_4 because of frustrated higher-order hopping[22]. Therefore, a key unanswered question is whether a 1 uc layer of La_2CuO_4 hosts a more resonating valence bond (RVB)-like state, or whether it obeys the expectations of the Heisenberg model with renormalized classical correlations. RVB-like models, shown as the dotted line in Fig. 2d, predict a much lower energy at $(\pi, 0)$ than at $(\pi/2, \pi/2)$ (ref. 11). In contrast, Fig. 2d shows no such downturn and, furthermore, our data imply the presence of similar magnetic correlations in single-layer and in bulk La_2CuO_4. Thus, our results strongly support the second scenario.

More specifically, our 1 uc data are consistent with the renormalized classical expectation for the Heisenberg model: even though theoretical work implies that thermal fluctuations suppress long-range order at any finite temperature in a perfectly two-dimensional system, in fact, as the temperature is lowered, the correlation length increases exponentially in $J/k_B T$ (ref. 14), the spin-wave lifetime likewise increases as correlation length divided by spin-wave velocity[23], and the system mimics a Néel state in its response. Neutron scattering studies of the nearest-neighbour material $Cu(DCOO)_2{\cdot}4D_2O$ have shown a small quantum correction to the magnon energy at $(\pi, 0)$ (refs 9,24). In contrast, our data show a 40 meV (13%) higher energy at $(\pi, 0)$ than at $(\pi/2, \pi/2)$, thereby confirming the neutron measurements on bulk La_2CuO_4 (refs 5,6). We conclude that even in the single La_2CuO_4 layer, the quantum corrections to the dispersion are small and hidden by a larger zone boundary dispersion due to the longer-ranged interactions resulting from higher-order hopping terms[5,6,19,22].

We are now in a position to study the 1 uc $S = 1/2$ response in detail. To do so, we first consider the bulk response (Fig. 3). A continuum of magnetic excitations is observed above the single-

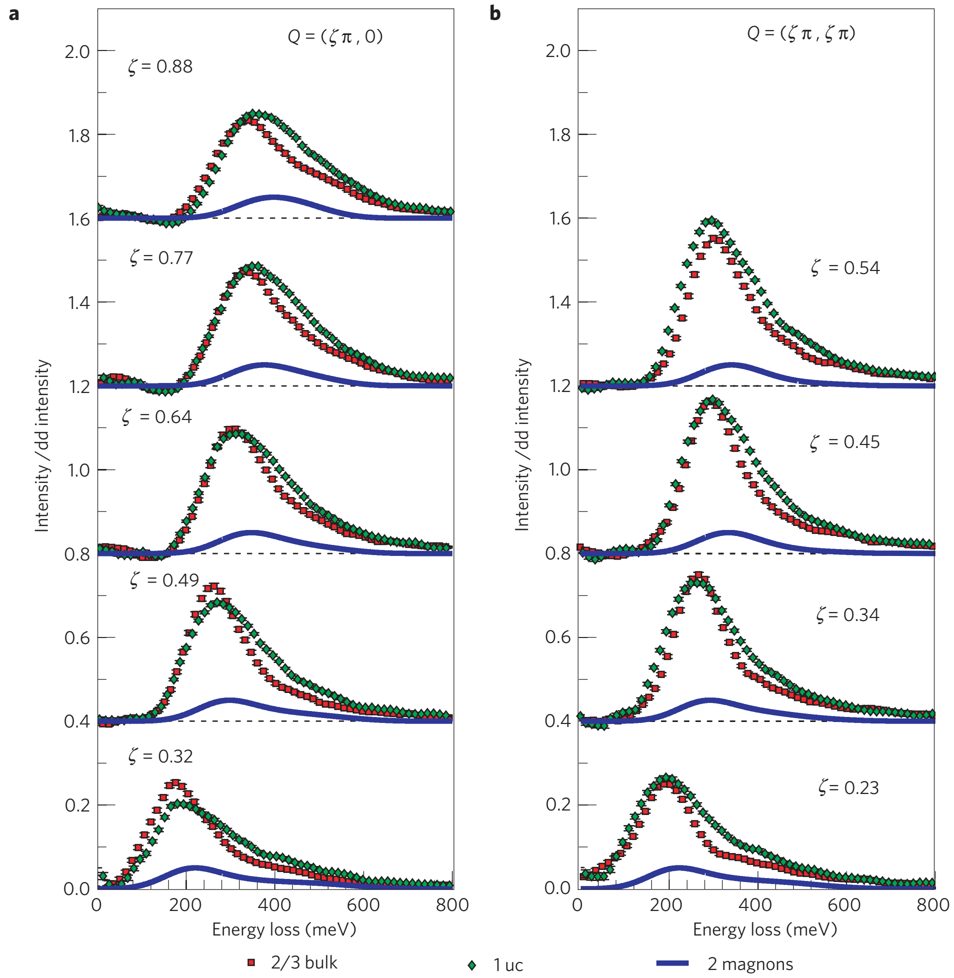

Figure 4 | Scaling of the magnetic excitations. a,**b**, A comparison between 2/3 of the bulk La_2CuO_4 response (red squares) and the 1 uc ($25 \times [LaAlO_3 + La_2CuO_4]$) response (green diamonds) along $(\zeta\pi, 0)$ (**a**) and $(\zeta\pi, \zeta\pi)$ (**b**). The difference between these spectra corresponds to the longitudinal magnetic response, to be compared to the two-magnon $S^{zz}(\mathbf{Q}, \omega)$ calculation (blue line)[22]. As it is not possible to measure absolute magnetic scattering intensities with RIXS at present, the calculation is shown with an arbitrary intensity.

magnon energy extending out to 800 meV, beyond which the tail of the *dd* excitations makes it hard to determine the origin of the scattering. Similar high-energy continua are seen at all momenta, as is evident from Fig. 2. We note that neutron scattering also sees high-energy magnetic scattering up to the maximum measured energy transfer of 450 meV (ref. 6). In Fig. 3, we see that this scattering is anisotropic; this high-energy weight is stronger near $(\pi, 0)$ than at $(\pi/2, \pi/2)$ relative to the magnon peak.

In first-order SWT, the magnons are fluctuations transverse (T) to the spin-quantization axis, and result in a resolution-limited magnon peak, with no weight at higher energies. Quantum fluctuations shift weight to a higher-energy continuum, which, within SWT, is longitudinal (L) two-magnon scattering. In addition, quantum Monte Carlo calculations[15] and neutron scattering[23] for a nearest-neighbour Heisenberg antiferromagnet have indicated a transverse continuum especially around $(\pi, 0)$. It has been speculated that this transverse continuum can in part be described as fractional spinon-like excitations[10,16]. There is also the possibility that part of this transverse continuum is three magnon processes, which RIXS may be sensitive to[25,26].

With this description of the bulk scattering in hand, we now turn to the 1 uc film. Comparing Fig. 2a and c we find that the 1 uc film shows a smaller peak intensity than the bulk and more spectral weight at high energies. As shown in refs 26–28, Cu *L*-edge RIXS, with σ polarized incident light, is dominated by the out-of-plane *c* axis magnetic response. In the bulk sample, magnetic moments order in the plane along the (110) axis, defining the spin-quantization axis. Thus, here RIXS measures the transverse response T. If the La_2CuO_4 layers in a 1 uc film are not long-range magnetically ordered, one might expect the domains of locally correlated spins to be randomly orientated either in or out of the CuO_2 planes. In this case, one then measures the isotropic response $2/3T + 1/3L$. Note that this scenario does not distinguish between slowly fluctuating patches of correlated spins (as expected within the renormalized classical model) and static, randomly oriented patches of correlated spins. Figure 4 compares the 1 uc spectrum to 2/3 of the bulk spectrum along (Fig. 4a) the $(\zeta\pi, 0)$ and (Fig. 4b) the $(\zeta\pi, \zeta\pi)$ symmetry directions. The 2/3 scaling factor results in similar heights of the single-magnon peak, which is known to be transverse. This validates our approach and shows that the domains of locally correlated spins are isotropic in spin space and not fixed in the plane. This allows us to distinguish transverse and longitudinal components, leading to two important observations: a large component of the continuum is present in both data sets, meaning that a large component is transverse in nature and therefore cannot be described as two-magnon scattering in SWT. At high energy transfers the 1 uc data show additional scattering, which must be longitudinal in nature. Unlike the continuum response measured in the bulk film, we observe no clear differences between $(0,0) \rightarrow (\pi, 0)$ and $(0,0) \rightarrow (\pi/2, \pi/2)$ for this additional scattering, which disperses to higher energies at higher **Q**. In a SWT picture, such additional longitudinal scattering would come from two-magnon $S^{zz}(\mathbf{Q},\omega)$ excitations. These are calculated for La_2CuO_4 (see Methods) and plotted for comparison in Fig. 4. We see that the two-magnon response does not accurately account for the additional scattering in the 1 uc magnetic excitation spectra.

The ratio of **Q**-integrated longitudinal to transverse scattering can be compared to calculations within SWT (ref. 29). For a Heisenberg magnet, this ratio is controlled by the spin reduction due to zero-point fluctuations $\Delta S = S - \langle S^z \rangle$, where $\Delta S = 0.2$ for $S = 1/2$ and then

$$\frac{\text{Longitudinal}}{\text{Transverse}} = \frac{\Delta S(\Delta S+1)}{(S-\Delta S)(2\Delta S+1)} \approx 0.6$$

We find that the mean weight of the additional scattering relative to the transverse scattering at the measured **Q** values is about 0.6, consistent with this estimate, although we note that our measured **Q** does not constitute a full integration over the zone.

The comparison of bulk and 1 uc La_2CuO_4 has revealed a longitudinal and transverse continuum in the magnetic excitation spectrum of La_2CuO_4, which has yet to be fully explained. Possibilities include transverse incoherent scattering[15], higher-order magnons[25,26] and the presence of proposed[16] spinon-like excitations in La_2CuO_4 (ref. 6). Alongside this, the clearly defined magnon dispersion in 1 uc La_2CuO_4 leads to the conclusion that even in a single unit cell of La_2CuO_4, the ground state hosts classical correlations rather than RVB-like quantum disorder and that these correlations can be probed by RIXS. Further theoretical and experimental studies are called for to explain our observations, and to determine whether these non-SWT features gain importance on doping and whether they are relevant to the mechanism of superconductivity in doped cuprates.

Methods

We performed our RIXS experiments at the ADRESS beamline at the Swiss Light Source using the SAXES instrument. The total fluorescence yield at the Cu L_3 edge was measured at regular intervals and the incident energy was tuned to the peak in the absorption. We determined the combined energy resolution of the monochromator and spectrometer by measuring the elastic scattering from carbon tape, which was well described by a Gaussian function with a full-width at half-maximum of 134 meV. The **Q** resolution was better than 0.004 Å^{-1}. The spectra were normalized to the intensity of the *dd* excitations to account for differing amounts of La_2CuO_4 probed in different films, and to facilitate the comparison of different films for a given scattering geometry. We denote the in-plane scattering vector, **Q**, using the tetragonal La_2CuO_4 unit cell $a = b = 3.8$ Å, with $\mathbf{Q} = (\pi, 0)$ parallel to the Cu–O–Cu bond direction.

For film synthesis, we employed a unique atomic layer-by-layer molecular-beam epitaxy system equipped with advanced tools for *in situ* surface analysis including reflection high-energy-electron diffraction and time-of-flight ion-scattering spectroscopy. Using this technique, we reproducibly fabricate single-crystal films with atomically smooth surfaces and interfaces as well as heterostructures and superlattices with superconducting or insulating layers that can be down to 1 uc thick[30,31]. Digital layer-by-layer growth and the capability to maintain atomic-scale smoothness were both crucial for the present study. The films were grown on single-crystal $LaSrAlO_4$ substrates, each with the 10×10 mm^2 surface polished perpendicular to the (001) direction, under 9×10^{-6} torr of ozone and at a substrate temperature of about 700 °C. The deposition rates were measured by a quartz crystal oscillator before growth and controlled in real time using a custom-made atomic absorption spectroscopy system. The quality of the film growth was checked by monitoring reflection high-energy-electron diffraction intensity oscillations, which provide digital information on the film thickness. The films were subsequently annealed under high vacuum conditions to drive out all of the interstitial oxygen and avoid inadvertent oxygen doping. The sample characterization described in the Supplementary Information shows that these films are a good realization of isolated 1 and 2 uc La_2CuO_4 layers.

The two-magnon excitation spectrum $S^{zz}(\mathbf{Q},\omega)$ was calculated following[22] for a Hubbard model relevant to La_2CuO_4. The first-, second- and third-nearest-neighbour hopping parameters were $t = 492$ meV, $t'' = -207$ eV and $t''' = -45$ meV, respectively[22], as determined by fitting to neutron scattering measurements[6]. The Coulomb repulsion was fixed at $U = 3.5$ eV.

Received 21 September 2011; accepted 26 July 2012; published online 2 September 2012

References

1. Hayden, S. M., Mook, H. A., Dai, P., Perring, T. G. & Dogan, F. The structure of the high-energy spin excitations in a high-transition-temperature superconductor. *Nature* **429,** 531–534 (2004).
2. Vignolle, B. *et al.* Two energy scales in the spin excitations of the high-temperature superconductor $La_{2-x}Sr_xCuO_4$. *Nature Phys.* **3,** 163–167 (2007).
3. Li, Y. *et al.* Hidden magnetic excitation in the pseudogap phase of a high-T_c superconductor. *Nature* **468,** 283–285 (2010).
4. Le Tacon, M. *et al.* Intense paramagnon excitations in a large family of high-temperature superconductors. *Nature Phys.* **7,** 725–730 (2011).
5. Coldea, R. *et al.* Spin waves and electronic interactions in La_2CuO_4. *Phys. Rev. Lett.* **86,** 5377–5380 (2001).
6. Headings, N. S., Hayden, S. M., Coldea, R. & Perring, T. G. Anomalous high-energy spin excitations in the high-T_c superconductor-parent antiferromagnet La_2CuO_4. *Phys. Rev. Lett.* **105,** 247001 (2010).
7. Braicovich, L. *et al.* Magnetic excitations and phase separation in the underdoped $La_{2-x}Sr_xCuO_4$ superconductor measured by resonant inelastic X-ray scattering. *Phys. Rev. Lett.* **104,** 077002 (2010).
8. Mermin, N. D. & Wagner, H. Absence of ferromagnetism or antiferromagnetism in one- or two-dimensional isotropic Heisenberg models. *Phys. Rev. Lett.* **17,** 1133–1136 (1966).
9. Christensen, N. B. *et al.* Quantum dynamics and entanglement of spins on a square lattice. *Proc. Natl Acad. Sci. USA* **104,** 15264–15269 (2007).
10. Anderson, P. W. The resonating valence bond state in La_2CuO_4 and superconductivity. *Science* **235,** 1196–1198 (1987).
11. Hsu, T. C. Spin waves in the flux-phase description of the $S = 1/2$ Heisenberg antiferromagnet. *Phys. Rev. B* **41,** 11379–11387 (1990).
12. Manousakis, E. The spin-1/2 heisenberg antiferromagnet on a square lattice and its application to the cuprous oxides. *Rev. Mod. Phys.* **63,** 1–62 (1991).
13. Keimer, B. *et al.* Magnetic excitations in pure, lightly doped, and weakly metallic La_2CuO_4. *Phys. Rev. B* **46,** 14034–14053 (1992).
14. Chakravarty, S., Halperin, B. & Nelson, D. Two-dimensional quantum Heisenberg antiferromagnet at low temperatures. *Phys. Rev. B* **39,** 2344–2371 (1989).
15. Sandvik, A. & Singh, R. High-energy magnon dispersion and multimagnon continuum in the two-dimensional Heisenberg antiferromagnet. *Phys. Rev. Lett.* **86,** 528–531 (2001).
16. Ho, C-M., Muthukumar, V., Ogata, M. & Anderson, P. Nature of spin excitations in two-dimensional Mott insulators: Undoped cuprates and other materials. *Phys. Rev. Lett.* **86,** 1626–1629 (2001).
17. Suter, A. *et al.* Two-dimensional magnetic and superconducting phases in metal–insulator $La_{2-x}Sr_xCuO_4$ superlattices measured by muon-spin rotation. *Phys. Rev. Lett.* **106,** 237003 (2011).
18. Schlappa, J. *et al.* Collective magnetic excitations in the spin ladder $Sr_{14}Cu_{24}O_{41}$ measured using high-resolution resonant inelastic X-ray scattering. *Phys. Rev. Lett.* **103,** 047401 (2009).
19. Guarise, M. *et al.* Measurement of magnetic excitations in the two-dimensional antiferromagnetic $Sr_2CuO_2Cl_2$ insulator using resonant X-ray scattering: Evidence for extended interactions. *Phys. Rev. Lett.* **105,** 157006 (2010).
20. Ament, L. J. P., van Veenendaal, M., Devereaux, T. P., Hill, J. P. & van den Brink, J. Resonant inelastic X-ray scattering studies of elementary excitations. *Rev. Mod. Phys.* **83,** 705–767 (2011).
21. Schlappa, J. *et al.* Spin-orbital separation in the quasi-one-dimensional Mott insulator Sr_2CuO_3. *Nature* **485,** 82–85 (2012).
22. Dalla Piazza, B. *et al.* Unified one-band Hubbard model for magnetic and electronic spectra of the parent compounds of cuprate superconductors. *Phys. Rev. B* **85,** 100508 (2012).
23. Rønnow, H. *et al.* Spin dynamics of the 2D spin 1/2 quantum antiferromagnet copper deuteroformate tetradeuterate (CFTD). *Phys. Rev. Lett.* **87,** 037202 (2001).
24. Singh, R. R. P. & Gelfand, M. P. Spin-wave excitation spectra and spectral weights in square lattice antiferromagnets. *Phys. Rev. B* **52,** R15695–R15698 (1995).
25. Ament, L. J. P. & van den Brink, J. Strong three-magnon scattering in cuprates by resonant X-rays, Preprint at http://arxiv.org/abs/1002.3773 (2010).
26. Igarashi, J-i. & Nagao, T. Magnetic excitations in l-edge resonant inelastic X-ray scattering from cuprate compounds. *Phys. Rev. B* **85,** 064421 (2012).
27. Ament, L., Ghiringhelli, G., Sala, M., Braicovich, L. & van den Brink, J. Theoretical demonstration of how the dispersion of magnetic excitations in cuprate compounds can be determined using resonant inelastic X-ray scattering. *Phys. Rev. Lett.* **103,** 117003 (2009).
28. Haverkort, M. W. Theory of resonant inelastic X-ray scattering by collective magnetic excitations. *Phys. Rev. Lett.* **105,** 167404 (2010).

29. Huberman, T. *et al.* Two-magnon excitations observed by neutron scattering in the two-dimensional spin-5/2 Heisenberg antiferromagnet Rb_2MnF_4. *Phys. Rev. B* **72,** 014413 (2005).
30. Gozar, A. *et al.* High-temperature interface superconductivity between metallic and insulating copper oxides. *Nature* **455,** 782–785 (2008).
31. Logvenov, G., Gozar, A. & Božović, I. High-temperature superconductivity in a single copper–oxygen plane. *Science* **326,** 699–702 (2009).

Acknowledgements
We thank R. Konik, M. Haverkort, A. Boothroyd and G. Luke for fruitful discussions, X. Liu for assistance with the sample characterization and S. Hayden and R. Coldea for sharing their data in ref. 6. The experiment was performed at the ADRESS beamline of the Swiss Light Source using the SAXES instrument jointly built by the Paul Scherrer Institut, Switzerland and the Politecnico di Milano, Italy. We acknowledge V. Strocov for support at the ADRESS beamline and A. Suter and T. Prokscha for their assistance with the muon spin rotation measurements. Work at Brookhaven National Laboratory was supported by the Office of Basic Energy Sciences, Division of Materials Science and Engineering, US Department of Energy under Award No. DEAC02-98CH10886. M.P.M.D. and J.P.H. are supported by the Center for Emergent Superconductivity, an Energy Frontier Research Center funded by the US DOE, Office of Basic Energy Sciences. C.M., K.J.Z and T.S. acknowledge support from the Swiss National Science Foundation and its NCCR MaNEP.

Author contributions
Experiment: M.P.M.D., J.P.H., R.S.S., C.M., K.J.Z. and T.S.; sample growth: I.B.; sample characterization: I.B., M.P.M.D., J.P., R.S.S. and E.M.; two-magnon calculations: B.D.P. and H.M.R.; data analysis and interpretation: M.P.M.D., J.P.H., J.v.d.B., T.S., C.M., K.J.Z. and H.M.R.; project planning: J.P.H., M.P.M.D., T.S. and I.B.; paper writing: M.P.M.D. and J.P.H., with contributions from all authors.

Additional information
Supplementary information is available in the online version of the paper. Reprints and permissions information is available online at www.nature.com/reprints. Correspondence and requests for materials should be addressed to M.P.M.D. or J.P.H.

Competing financial interests
The authors declare no competing financial interests.